

An Assessment of Antarctic Sea-ice Thickness in CMIP6 Simulations with Comparison to the Observations

Shreya Trivedi¹, Will Hobbs², and Marilyn Raphael¹

¹Department of Geography, University of California, Los Angeles

²Australian Antarctic Program Partnership, Institute for Marine and Antarctic Studies, University of Tasmania, nipaluna/Hobart, Australia.

Corresponding author: Shreya Trivedi (shreyatrivedi26@ucla.edu)

Key Points:

- CMIP6 models can capture the timing of annual cycle (particularly in February) and spatial patterns of SIT resembling the observations.
- Compared to sea-ice area, CMIP6 models exhibit larger negative biases in thickness/volume, with a higher degree of variation among models.
- Seasonal variations in sea-ice show positive (negative) relationships between sea ice area and thickness during September (February).

Abstract

This study assesses less-explored Southern Ocean sea-ice parameters, namely Sea-ice Thickness and Volume, through a comprehensive comparison of 26 CMIP6 models with reanalyses and satellite observations. Findings indicate that models replicate the mean seasonal cycle and spatial patterns of sea-ice thickness, particularly during its maxima in February. However, some models simulate implausible historical mean states compared to satellite observations, leading to large inter-model spread. September sea-ice thickness is consistently biased low across the models. Our results show a positive relationship between modeled mean sea-ice area and thickness in September (i.e., models with more area tend to have thicker ice); in February this relationship becomes negative. While CMIP6 models demonstrate proficiency in simulating Area, thickness accuracy remains a challenge. This study, therefore, highlights the need for improved representation of Antarctic sea-ice processes in models for accurate projections of thickness and volume changes.

Plain Language Summary

In this study, we investigated sea-ice thickness and volume in the Southern Ocean using data from 26 different climate models and observation datasets. Our findings show that the models generally capture the seasonal cycle and spatial patterns of sea-ice thickness well, with the highest average thickness occurring in February. We also found that the models tend to perform better in simulating sea-ice area compared to thickness. Furthermore, simulated sea-ice area and thickness tend to behave differently during different seasons—positively (negatively) covarying in September (February). The models that performed well in simulating sea-ice area faced challenges in accurately representing thickness and volume. This raises the question regarding the overall performance of such models or, more definitively, whether it's reliable to evaluate model accuracy or performance based solely on sea-ice area. Nevertheless, sea-ice thickness simulations in CMIP6 can offer a basis for initial analyses of absolute sea-ice changes in the Southern Ocean, despite the need for more reliable observational thickness.

1. Introduction

Antarctic sea-ice extent, which showed a small positive linear trend since the start of satellite era (Cavalieri & Parkinson, 2008; Parkinson & Cavalieri, 2012; Turner et al., 2015; Zwally et al., 2002), has decreased significantly since mid-2016 (Raphael and Handcock, 2022; Wang et al., 2022; Turner et al., 2022; Eayrs et al., 2021). Attempts to understand this variation have focused primarily on the surface characteristics (extent and area) of the ice. Variability in sea-ice thickness (SIT) and volume (SIV) have not been explored and this is due to limited SIT observations. However, complete understanding of the changes in sea-ice and their potential impact on climate is not possible if these variables are not examined. For example, SIV serves as a measure of total sea-ice production and, hence, a measure of the surface salinity flux in winter, the freshwater input to the ocean in summer, and total heat loss to the atmosphere. This further aids our understanding of surface buoyancy flux and related ventilation of SO deep waters (Pelichero et al., 2018) hence by inference, global ocean heat and carbon uptake. Detection of variations in SIT/SIV are also important for understanding a variety of climate-sea-ice feedbacks (Holland et al., 2006; Stammerjohn et al., 2008) as well as trends and variability in SO salinity (Haumann et al., 2016). Therefore, a long-term assessment of these variables is important for a

complete assessment and quantification of the ongoing changes in the mass balance of the sea-ice cover (Massonnet et al., 2013) allowing for a deep propagation of the global climate change signal (Sallée et al., 2023).

Accurate simulations of long-term SIT are also important for understanding the marine biology of the Antarctic ecosystem. SIT affects the maximum biomass of algae in different ice layers, which in turn influences the food web of the SO. SIV along with the snow depth, also affects the light penetration and availability for the phytoplankton contributing further in their production and bloom (Massom & Stammerjohn, 2010; Schultz, 2013). Therefore, a comprehensive assessment of Antarctic sea-ice variability and its impact on the ocean requires an additional consideration of the SIT and SIV (Maksym et al., 2012; Maksym & Markus, 2008).

Global coupled climate models (GCMs) are potentially valuable tools for assessing long-term SIT and SIV variability and providing future projections. However, the simulation of Antarctic sea-ice, particularly SIT in GCMs, remains a challenge, adding to the *low confidence* in Antarctic sea-ice projections (Meredith et al., 2019). Here, we present a high-level evaluation of models in the Sixth Coupled Model Intercomparison Project (CMIP6; Eyring et al., 2016) in simulating Antarctic SIT/SIV and compare them to available observations. Our findings indicate that models can reasonably capture the timing of SIT seasonal cycle, although some biases and model disagreements are evident. However, when compared to SIA, their performance remains suboptimal.

2. Data and Methods

2.1. Observation Datasets

Our study uses three different observational records for SIT: Satellite dataset Envisat-CryoSat-2 (2002-2012), the Global Ice-Ocean Modeling and Assimilation System (GIOMAS, 1979-2014) and the German contribution to the Estimating the Circulation and Climate of the Ocean project (GECCO3, 1979-2014). The satellite dataset is used as the comparison baseline.

SIT from Envisat and Cryosat-2:

The Sea-Ice Climate Change Initiative (SICCI) project provides a large-scale Antarctic SIT dataset from Envisat and CryoSat-2 with a 50 km spatial resolution (Hendricks et al., 2018). While these SIT products have uncertainties due to radar altimeter estimates (Paul et al., 2018; Tilling et al., 2019; Willatt et al., 2010), they offer valuable insights. Previous studies have shown reasonable regional agreement between Envisat and CryoSat-2 radar freeboards (Schwegmann et al., 2016), although Envisat tends to overestimate ice thickness (Shi et al., 2021) particularly in the Antarctic (Hendricks et al., 2018a; Hendricks et al., 2018b; Wang et al., 2022). Despite these challenges, the SICCI dataset remains the most comprehensive satellite dataset available, covering the circumpolar Antarctic SIT from 2002 to present. Envisat and CryoSat-2 have been found comparable to Upward Looking Sonar (ULS)-derived SIT for the Weddell region (Shi et al., 2021; Liao et al., 2022; Wang et al., 2022) and also aligns well with in-situ ship-based observations, (ASPeCt; Worby et al., 2008) which showed highest thickness in summers and lowest in autumn-winter. These agreements can help refine and assess model performance, particularly in capturing the seasonal cycle of SIT.

SIT from sea-ice estimates and reanalysis:

The GECCO3 ocean synthesis, an improved version of GECCO2 based on MITgcm, employs the adjoint method to fit the model to various data over a multidecadal period, providing a global eddy-permitting synthesis at a resolution of 0.4° (Köhl, 2020). The Global Ice-Ocean Modeling and Assimilation System (GIOMAS) uses the Parallel Ocean Model coupled with a 12-category thickness and enthalpy distribution ice model at a horizontal resolution of 0.8° (Zhang & Rothrock, 2003). GIOMAS assimilates sea-ice concentration, demonstrates good agreement of its SIT (Lindsay & Zhang (2006) with satellite observations in the Arctic and is useful for studying long-term variations in Antarctic sea-ice (Liao et al., 2022; Shi et al., 2021). To make reanalysis products comparable to absolute floe thickness estimates (the SIV per grid-cell area or “equivalent sea-ice thickness”), we convert them into “effective thicknesses” by dividing them with observed SIC records from the National Snow and Ice Data Center (NSIDC) (Cavalieri et al., 1999) by re-gridding the SIT to the concentration grid.

2.2. CMIP6 Models

In our study, we analyze the historical experiments of the CMIP6 dataset, specifically focusing on the “*sithick*” variable, representing simulated effective floe thickness. We also incorporate “*siconc*” (sea-ice concentration) and “*areacello*” (area of individual grid cells over the ocean) variables. CMIP6 models generate multiple ensemble members, which are multiple runs or simulations with slightly different initial conditions or variable settings, used to capture uncertainty and variability in model predictions. In this study, we consider the first ensemble member for each model (Table S1) to account for internal variability and ensure consistency (Notz & Community, 2020; Roach et al., 2020). We calculate SIV by multiplying “*siconc*”, “*sithick*” and “*areacello*” and summing over the circumAntarctic SO. For SIA, we multiply “*siconc*” and “*areacello*” and integrate it over the circumAntarctic SO. Lastly, for floe thickness, we use the averaged “*sithick*” over SO.

3. Results

3.1. Sea-ice variables: Mean and Anomaly State

Fig.1 shows the 2002-2014 mean annual cycles of SIV, SIT, and SIA in different observational estimates and CMIP6 models. As mentioned earlier, the Envisat-CryoSat2 observations (henceforth referred to as satellite product) are known to have high positive biases especially in the Southern Hemisphere (SH); thus, anomalously high volume (Fig.1a) and thickness (Fig.1b). The multi-model mean (MMM) is much smaller than the satellite and reanalysis products for SIA and SIV, whereas in SIT most of the models simulate thicker sea-ice than the reanalyses between January-April. However, all the models can simulate the SIV maxima (Sept-Oct) and minima (Feb) and the SIT maxima (Feb), while simulated SIT minima fall in April at the start of the growing period (like the reanalyses).

Previous studies have shown that CMIP6 models perform well in simulating SIA climatology in the circumAntarctic (Roach et al., 2020; Shu et al., 2020). Significant negative biases are consistently observed in SIV (Fig.1a). However, for SIT during summer, the outcomes vary considerably based on the observation dataset, with certain models simulating unusually thick sea-ice ($>3\text{m}$) in January-February (Fig.1b). This summer biases can be attributed to the increased complexity in satellite retrieval of summer SIT (Kurtz & Markus, 2012).

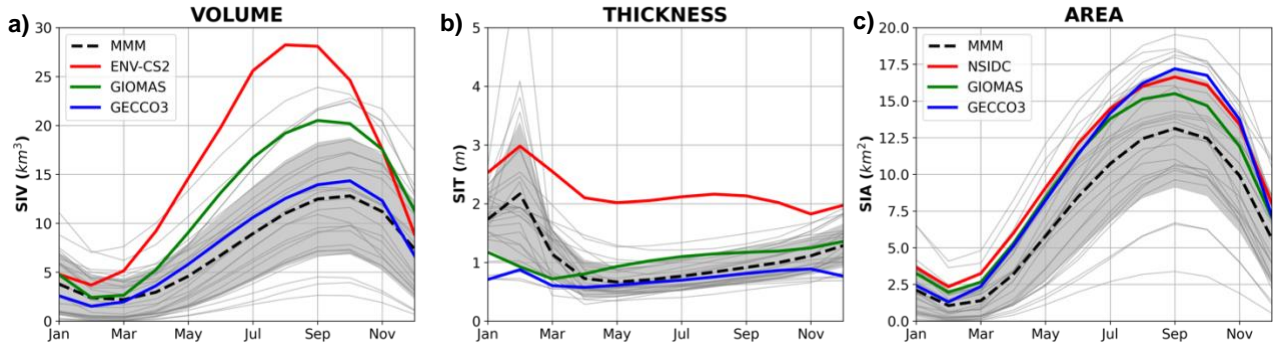


Fig. 1: Comparison of annual cycles of SIV, SIT and SIA of the circumpolar Antarctic. All the CMIP6 models are shown as grey lines, The Multi-Model Mean (MMM) is the black dashed line. GECCO3 in blue, GIOMASS in green, and Envisat-CryoSat-2/NSIDC in red. Grey shaded areas are ± 1 standard deviation for the MMM.

There is a similar pattern in the SIA (Fig.1c) cycles except a few models which tend to simulate larger SIAs during the entire cycle particularly between July and November. The inter-model spread of annual mean Antarctic SIT, SIV and SIA is 5.9m, 20 thousand km³ and 16 million km² for the maxima and 1.8m, 7.5 thousand km³ and 4 million km² for the minima, respectively. Inter-model spread however fluctuates and is larger during fall and winter for SIV and SIA while it greatly reduces during the summers. By contrast, SIT has greater inter-model spread during summers and shrinks significantly from April-November. Among the observation datasets, all variables show the highest spread during the cooler seasons.

The highest average thickness of ice in the SO occurs in February in the form of the compacted ice which survives the melt season (Kurtz & Markus, 2012; Worby et al., 2008; Xu et al., 2021). It is for this reason that the SIT seasonal cycles look very different from those of SIA/SIV. Therefore, to capture the sea-ice seasons based exclusively on the SIT climatology, we conducted our analyses using February and September.

Previous studies have shown that CMIP6 models struggle to reproduce the observed positive trend in Antarctic sea-ice extent (SIE) and SIA (Li et al., 2023; Shu et al., 2015; Turner et al., 2013). The negative trends in simulated SIT/SIV (Fig.S1) are consistent with the negative trends in SIE/SIA (Roach et al., 2020 and Shu et al., 2020). However, no significant trends were found in modeled and observed SIT in February with only a weak negative trend in the MMM of SIV, which can be potentially attributed to the simulated negative trend in SIA. This negative trend becomes stronger in the early 2000s, particularly in September (similar to trends in Shu et al., 2020).

We conducted a similar analysis over the four seasons and observed seasonal variability in sea-ice (Fig. S2). There were significant SIT/SIV trends apparent during the cooler seasons (winter and spring), while such trends were absent in the warmer seasons. On the contrary, studies have shown the observed SIA trends are primarily observed in the warmer seasons (Summer and Fall) because the maximum ice edge is constrained by SO hydrography, while they remain absent during the cooler seasons (Eayrs et al., 2019; Hobbs et al., 2016). This implies that changes in SIT/SIV may contribute to Antarctic sea-ice variability during colder months. The presence of robust land-ocean temperature gradients during winters may be a contributing mechanism here

because they result in high-intensity winds, which are recognized as significant contributors to SIT/SIV fluctuations in the SO (Zhang, 2014).

3.2. CMIP6 Model Performance

An accurate spatial distribution of SIT is key to estimates of SIV and it reflects the skill in simulation of local processes, coupled interactions and energy transfer among the ocean below, the sea-ice, and the atmosphere above (Stroeve et al., 2014). To estimate this, we computed spatial pattern correlations and Root Mean Square Deviations (RMSD) for the sea-ice variables among 26 models, the reanalyses, and the satellite product. These calculations were performed based on area-integrated spatial averages of sea-ice over February and September, using data subsets for models and observations corresponding to those months. We utilized the satellite dataset as the reference for calculating RMSD and correlation values across spatial grids. The values plotted on the Taylor Diagram (Fig.S3) represent the spatial average of the correlation coefficient, RMSDs and standard deviations across the circumpolar Antarctic.

Higher correlation coupled with a lower RMSD represents greater accuracy of CMIP6 models in simulating the sea-ice variables. Fig.S3 shows that most of the models have a lower RMSD for SIA (Fig.S3c,d) compared to SIV and SIT. Out of all the variables, models tend to have highest RMSDs for the SIT (Fig.S3a,b) with almost all the models with their values between 0.5-1.0 during both months. The reanalysis products show the highest RMSDs and lowest correlations for SIT, indicating lack of agreement among different observations, while a contrasting pattern is seen for SIA (Fig.S3e,f). Comparing the two months, we observe that RMSDs are smaller for September, most notably in SIA and SIV. For SIT, models tend to perform better for the SIT maxima in February (Fig.S3a). Spatial correlation coefficients range between 0.6-0.9 for all the variables in both the months (Table S2, S3 and S4). NorCPM1, MRI-ESM2-0, SAM0-UNICON, CESM2-WACCM-FV2, and CESM2-FV2 demonstrate highest correlations for SIA. For SIV, NorCPM1, MRI-ESM2-0, and SAM0-UNICON perform well, while MPI-ESM1-2-LR, MPI-ESM1-2-HR, MPI-ESM1-2-HAM, and ACCESS-CM2 show high correlations for SIT in both months. In summary, the Taylor Diagram reveals that while most CMIP6 models demonstrate relatively higher accuracy in simulating SIA and SIV with strong correlations and lower RMSD, they face greater challenges in accurately reproducing SIT, particularly during September. Additionally, the reanalysis products exhibit lower agreement and higher RMSD for SIT, emphasizing the complexity of capturing this variable across different observation datasets.

Given their better performance in simulating SIA, we considered whether or not this performance correlated with SIT accuracy in CMIP6 models. For this, we compared the annual averages of SIT and SIA in models with the observations (Fig.2). SIA biases look similar in both the months with their values ranging between -1.3 to -2.0 million km². On the other hand, SIT consistently exhibits thin biases across all models for September ranging between 1-2m (Fig.2b). February is also characterized by thinner sea-ice simulations (most models in Fig.2a have values less than observed value of 3m) except a few models which show a good agreement with the observations (models with their average SIT ~3m).

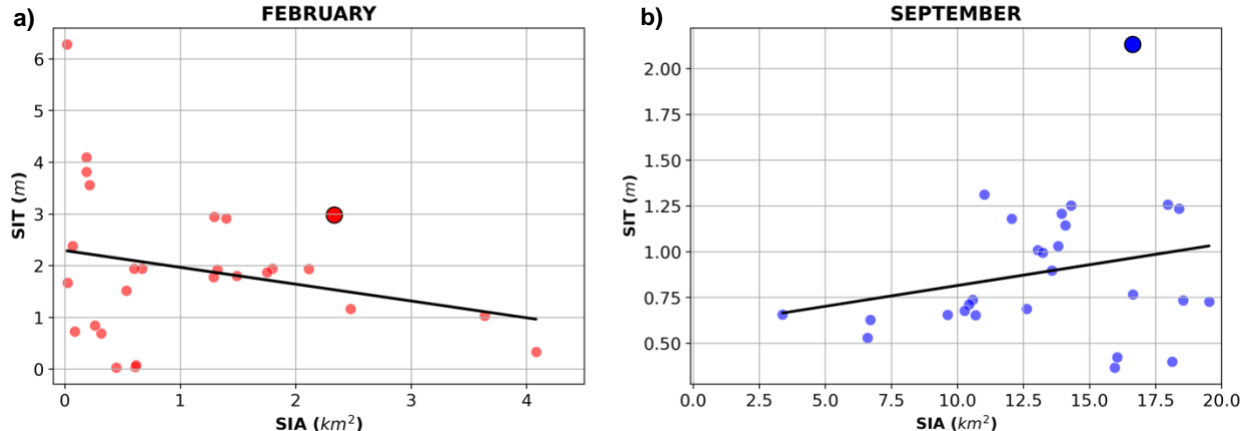


Fig. 2: Scatter plots between the annual means of SIT (y-axis) and SIA (x-axis) for CMIP6 models and Observations for the period (2002-2014) for February (red) and September (blue). The line of best fit represents the relationship between the two variables for selected months. Each small dot represents a model while the larger dots represent observations (ECS2 and NSIDC for SIT and SIA, respectively). The figure clearly demonstrates seasonal variations in magnitudes of both the variables.

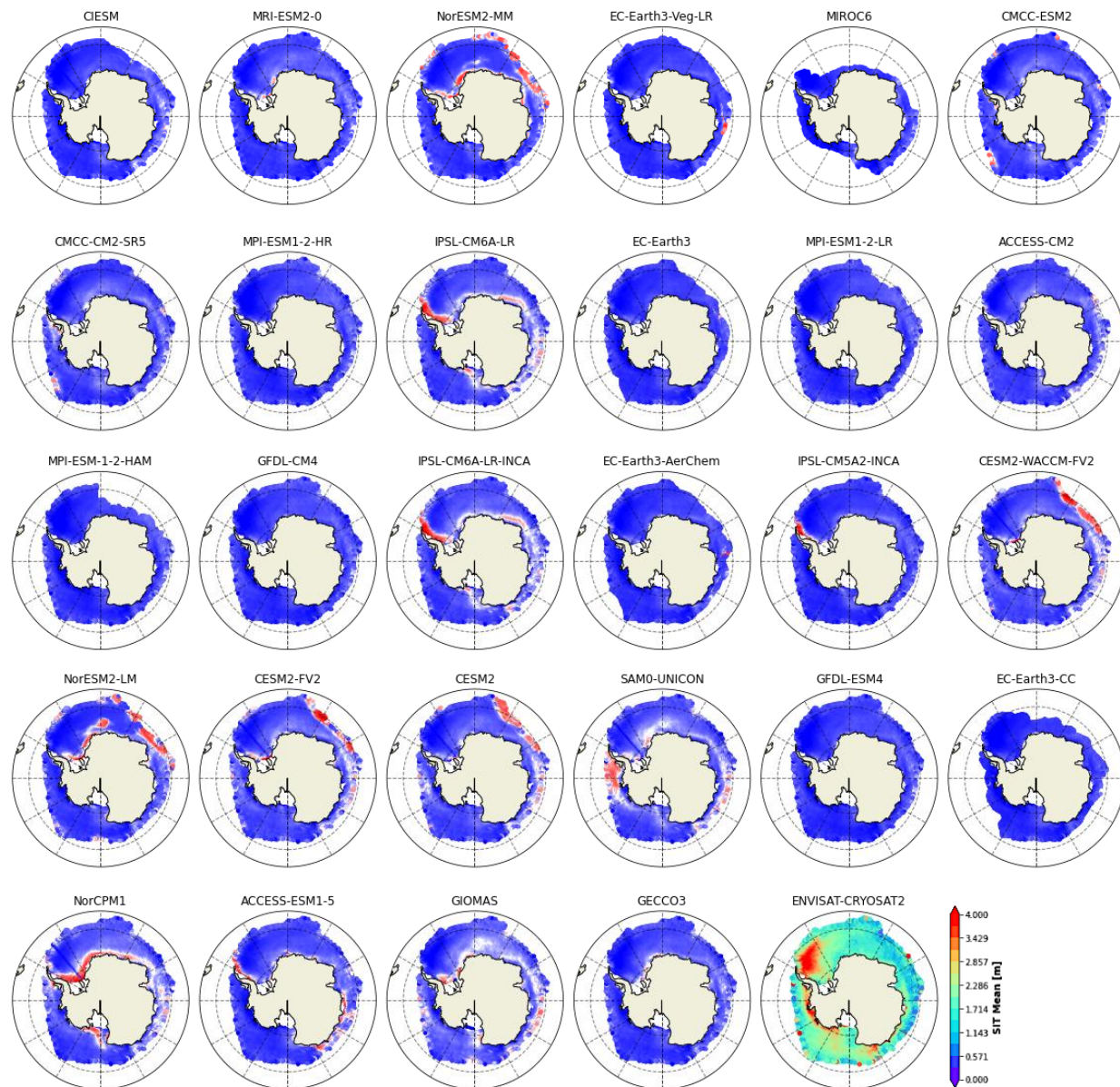
We anticipate consistency in model simulations and responses for the sea-ice variables, so that smaller SIA, would be accompanied by thinner SIT as most areas will be covered with thin first year ice. However, some models exhibit contrasting behaviors. In February, EC-Earth3 models display positive biases in SIT (with SIT > 3m in Fig.2a) and negative biases in SIA. In September, models like MRI-ESM2-0, SAM0-UNICON, NorCPM1, IPSL-CM6A-LR, and IPSL-CM6A-LR-INCA simulate thinner sea-ice along with positive biases in SIA (with values greater than 17.5 km² in Fig.2b). This intriguing behavior raises questions about the accuracy and reliability of these models in simulating sea-ice variables. These opposing relationships may be due to some intricate thermodynamic relationships between SIA and SIT captured by the models or to model errors. Further study might clarify this.

Fig.2 also highlights how simulated seasonal means in SIA and SIT behave differently—with positive (negative) correlation occurring during September (February). This could happen as increasing temperatures during summers result in sea-ice melt thereby reducing SIA with the thickest of the sea-ice surviving the melt season, hence an inverse relationship in February. A positive correlation is observed between SIA and SIT during the growing season when temperatures are decreasing. These thermal changes lead to increases in both area and thickness, with SIT increasing but remaining relatively thinner as SIA expands. Consequently, Area and Thickness “positively covary” with reduced temperatures.

3.3. Spatial patterns and biases

Compared to other sea-ice variables, simulated SIT shows a noticeable agreement among models during February. Despite the agreement, it is necessary to acknowledge the substantial level of uncertainty that exists regarding the accuracy of SIT simulation due to heterogeneity among various models. This variability is manifested in the significant inter-model disparity as well as marked differences in the spatial distribution of thickness across the SO (Fig.3 and Fig. S4). The mean observed SIT in the satellite product shows that thickest sea-ice is in the Weddell

Sea along the Antarctic Peninsula and along the coastal edges of the Amundsen-Bellingshausen Seas (ABS)--the ice which survives the summer melt. There is relatively thinner sea-ice observed on the eastern Antarctic (Kurtz & Markus, 2012). Our analysis reveals that most of the CMIP6 models capture a similar spatial pattern in SIT around the Antarctic. However, they do exhibit negative biases and underestimate thickness primarily along the Peninsula in Weddell and in the ABS. Some models simulate a thicker sea-ice compared to the observations (Fig.S4) around the tip of the Peninsula (IPSL-CM6A-LR, IPSL-CM6A-LR-INCA and IPSL-CM5A2-INCA), between the western edge of the ABS and Ross Sea (EC-Earth3 models), around the coast of ABS (SAM0-UNICON) and western Weddell Sea region (NorCPM1). It is probably this thickness in sea-ice along Peninsula in the Weddell region which contributes to a high spatial correlation value between such models and satellite observations in February.



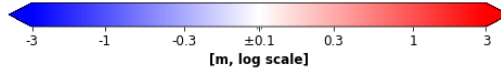


Fig. 3: Spatial Biases of SIT averaged over 2002 to 2014 (September) for 26 CMIP6 models and Reanalyses from the reference dataset: ENVISAT-CS-2. Last figure shows the time averaged SIT for ENVISAT-CS-2.

The spatial distribution patterns of SIT during September (Fig.3) bear similarities to February, with thickest multi-year sea-ice in the Weddell. Here, we find anomalously thick ice (>3m) in some CMIP6 models primarily in *two* regions: an elongated *tongue of thickest sea-ice* extending northward from the northwest Weddell Sea along the AP and, the other is *around the sea-ice edge*. Multiple models, including IPSL-CM6A-LR, IPSL-CM6A-LR-INCA, IPSL-CM5A2-INCA, EC-Earth3-Veg-LR, EC-Earth3-AerChem, NorCPM1, and ACCESS-ESM-1-5, show a similar tongue of thick sea-ice that also agrees with observed patterns (consistent with ICESat measurement by Holland & Kwok, 2012 and modeled SIT by Holland, 2014). The distinctive tongue-like pattern, characterized by clockwise ice motion, is a due to a prominent feature in the Weddell Sea called the *Weddell Gyre* (Vernet et al., 2019). This mechanism contributes significantly to the regional sea-ice dynamics in the form of an apparent westward ice motion in the southern Weddell. As a result, ice convergence occurs in the southwestern Weddell causing dynamic thickening (Shi et al., 2021). The sea-ice velocity vectors showed that CMIP6 models tend to capture this gyre (not shown) which results in the formation of a thick ice along the Peninsula.

Another potential explanation for the prominent sea-ice tongue is the influence of fast-ice in the Weddell (i.e., sea-ice that is pinned to the coast or grounded icebergs, Fraser et al 2023), a feature often inadequately represented or omitted in GCMs. Some sea-ice models have previously used prescribed fast-ice, either through a constant SIT over a specific region, or by setting its velocity at zero to render the blocking of sea-ice advection by sub grid-scale grounded icebergs (Kusahara et al., 2017; St-Laurent et al., 2017). Recent high-resolution regional NEMO-LIM-based experiments exhibited overestimations of SIT by 30-50% (compared to the satellite altimetric sea-ice products) during Winter and Fall within the fast-ice zone, indicating the presence of thicker ice, particularly in dynamically formed fast-ice areas (Van Achter et al., 2022). Interestingly, the CMIP6 models examined in our study, which demonstrate thicker coastal SIT around the Peninsula, utilize NEMO-LIM as their sea-ice model (Table S1 and Fig.3). Such thicknesses are far in excess of that expected from heat loss to the atmosphere alone, indicating likely contributions from platelet accretion and/or snow-ice formation hinting at the presence of fast-ice (Fraser et al., 2023).

The other region of thick sea-ice bias is the sea-ice edge (Fig.3). It's interesting to note that the CMIP6 models that have exhibited better performance in simulating Antarctic SIA such as CESMs, NorESM2, and ACCESS (Holmes et al., 2019; Li et al., 2023; Roach et al., 2020; Uotila et al., 2014) and showed lower thickness biases in February, simulate very high thickness at the sea-ice edge (between 0-70°E). A potential explanation for this could be through combinations of changes in air-ice drag and the direction of cold or warm-air advection. These may result in northward wind stress causing the sea-ice to drift, transport and accumulate causing dynamic convergence at the sea-ice edge (Singh et al., 2021; Holland et al., 2014; Holland & Kwok,

2012). Another reason could be the high-intensity ocean-wave fields linked to the SO which deeply infiltrate the sea-ice marginal ice zone. This penetration induces alterations in thickness distribution through processes like rafting and ridging, especially in the vicinity of the ice edge (Langhorne et al., 1998). In any case, the simulated sea-ice at the ice edge is much thicker than observed and further study is required to eliminate modeling error as its cause.

Overall, CMIP6 models simulations compare favorably with satellite-derived SIT observations during February (Fig.S4). About 38% of the CMIP6 models (10 out of 26) have their mean biases between $\pm 1\text{m}$. Among them, NorESM2-MM, CESM2-Models, and CMCC-ESM2 while spatially consistent with the observations display some biases. In general, all models tend to underestimate SIT and produce relatively thinner sea-ice during both months. These negative biases are more pronounced in September and reduce considerably in February. It should be kept in mind that our comparisons are made with respect to the satellite dataset which themselves exhibit an exaggerated SIT in the SO. Therefore, the 7 out of 26 models which show even greater positive biases ($>1\text{m}$), may be simulating unrealistic and excessively thick sea-ice in the SO and may represent a false picture of future Antarctic sea-ice changes.

4. Conclusions

Given the current context of global warming, it is imperative to develop predictions regarding Antarctic sea-ice behavior to enhance our understanding of its future variability and response to climate change. For this we need reliable estimates of SIT and SIV to assess the absolute changes in the global sea-ice. While there is the understanding that the models do not yet accurately simulate SIT and SIV, it is still necessary to see how well they perform if only to understand where more work is needed. The research presented here is a comprehensive evaluation of Antarctic SIT/SIV by comparing 26 model outputs with satellite data as a reference baseline. It is difficult to estimate and simulate SIT accurately due to the lack of long-term, reliable observational datasets. However, despite these limitations, CMIP6 models can offer longer timescales of SIT data which when compared with the observed (and accounting for the limitations), can enhance our understanding of Antarctic sea-ice.

Regardless of simulation of processes or trends, a precise modeling of climatological mean sea-ice cover in the GCMs is a necessary condition for accurate projections (Holmes et al., 2022). In line with this, our study shows that most models can simulate the timing of annual cycles of SIT/SIV. Additionally, in February, the SO retains the thickest sea-ice, consisting of sea-ice that survives the summer, which is also effectively captured by CMIP6 models. Modeled seasonal cycles for SIV and SIA show significant biases in April-October, with higher inter-model spreads in fall-winter. Conversely, SIT inter-model spreads are higher during November-March but exhibit relatively lower biases compared to the reference dataset. It should be noted that simulations without data assimilation are always out of phase with natural variability seen in the observations. Hence, these differences between simulations and observations can either be due to model biases or natural climate variability (Stroeve et al., 2014).

CMIP6 models continue to simulate negative trends in Antarctic SIT/SIV, contrary to the observed positive trends, until 2014. Additionally, we observe positive trends in SIT/SIV during cooler seasons (which are absent in SIA) implying that sea-ice variability in these colder months

could be influenced by thickness/volume changes, possibly due to intensified seasonal winds. Among the models, MRI-ESM2-0, CESM2, and ACCESS-CM2 demonstrate higher correlations and relatively lower RMSDs across all variables during both months. An evaluation of model biases demonstrates that SIA exhibits least biases compared to SIV and SIT, with better alignment observed in February. We also examined seasonal variations in sea-ice correlations, showing positive(negative) relationships between SIA and SIT during September(February). Certain models simulate opposing biases for SIT and SIA, revealing discrepancies between modeled simulations of these two variables and their responses to the model processes.

While many CMIP6 models simulate spatial SIT patterns like observations, they tend to underestimate SIT particularly in September. Intriguingly, certain models display anomalously thick sea-ice along the Peninsula and on the eastern sea-ice edges even greater than the exaggerations in reference dataset itself.

Such deviations can hamper our understanding of climate-sea-ice interactions as well as biological feedback between the oceans and climate. For instance, lower SIT could potentially create a misleading impression of lower albedo and increased light penetration, subsequently leading to increased Primary Production (Jeffery et al., 2020) and lower ocean acidification. We have not explored the causes of such anomalous biases in SIT. However, their potential explanations may include cloud effects (Kay et al., 2016; Zelinka et al., 2020), spatial resolution that does not permit eddies, which are understood to be highly important for representation of SO dynamics (Poulsen et al., 2018; Rackow et al., 2019), models treating all sea-ice to be able to drift when in reality up to 15% of ice should be held still either being anchored to land or grounded icebergs (Fraser et al., 2023) and the lack of coupled ice sheet interactions, which have relevance for the entire Antarctic climate system (Bronselaer et al., 2018; Golledge et al., 2019; Purich & England, 2023).

Considering these findings, we anticipate that future studies will investigate these aspects with respect to Antarctic SIT. Addressing such model biases could be initial steps in further improving the representation of dynamic processes in sea-ice, climate, and biogeochemical models, ensuring their accurate predictions. Understanding biases in sea-ice parameters and physical mechanisms behind these constraints will improve the reliability of sea-ice projections and increase confidence in our understanding of what controls the rate of Antarctic sea-ice loss. Therefore, our research addresses a critical knowledge gap of understanding and modeling of Antarctic SIT and the dynamics involved in shaping its temporal and spatial distributions using the long-term coupled climate simulations.

Acknowledgement

M.R. Raphael and S. Trivedi acknowledge funding by the National Science Foundation (NSF) under the Office of Polar Programs (NSF-OPP-1745089). W.R. Hobbs acknowledges support by the Australian Government as part of the Antarctic Science Collaboration Initiative program and receives funding from the Australian Research Council Discovery Project (DP230102994).

Data Availability Statement

The satellite product used in the study is CryoSat-2 and Envisat sea-ice thickness data which is available at <https://dx.doi.org/10.5285/b1f1ac03077b4aa784c5a413a2210bf5> (Hendricks et al., 2018). The GECCO3 sea-ice thickness data are available at <https://www.cen.uni-hamburg.de/en/icdc/data/ocean/easy-init-ocean/gecco3.html> (last access: 31 May 2021, Köhl, 2020). The GIOMAS sea-ice thickness data are available at http://psc.apl.washington.edu/zhang/Global_seoice/data.html (last access: 26 December 2020, Zhang and Rothrock, 2003). Monthly values of sea-ice concentration from NSIDC are available at <https://doi.org/10.5067/7Q8HCCWS4IOR>. All the CMIP6 model datasets are available at ESGF website: <https://esgf-node.llnl.gov/search/cmip6/> (Table S1).

References

- Bronsemaer, B., Winton, M., Griffies, S. M., Hurlin, W. J., Rodgers, K. B., Sergienko, O. V., Stouffer, R. J., & Russell, J. L. (2018). Change in future climate due to Antarctic meltwater. *Nature*, 564(7734), Article 7734. <https://doi.org/10.1038/s41586-018-0712-z>
- Cavalieri, D. J., & Parkinson, C. L. (2008). Antarctic sea ice variability and trends, 1979–2006. *Journal of Geophysical Research: Oceans*, 113(C7). <https://doi.org/10.1029/2007JC004564>
- Eayrs, C., Holland, D., Francis, D., Wagner, T., Kumar, R., & Li, X. (2019). Understanding the Seasonal Cycle of Antarctic Sea Ice Extent in the Context of Longer-Term Variability. *Reviews of Geophysics*, 57(3), 1037–1064. <https://doi.org/10.1029/2018RG000631>
- Eayrs, C., Li, X., Raphael, M. N., & Holland, D. M. (2021). Rapid decline in Antarctic sea ice in recent years hints at future change. *Nature Geoscience*, 14(7), 460–464. <https://doi.org/10.1038/s41561-021-00768-3>
- Eyring, V., Gleckler, P. J., Heinze, C., Stouffer, R. J., Taylor, K. E., Balaji, V., Guilyardi, E., Joussaume, S., Kindermann, S., Lawrence, B. N., Meehl, G. A., Righi, M., & Williams, D. N. (2016). Towards improved and more routine Earth system model evaluation in CMIP. *Earth System Dynamics*, 7(4), 813–830. <https://doi.org/10.5194/esd-7-813-2016>
- Fraser, A. D., Wongpan, P., Langhorne, P. J., Klekociuk, A. R., Kusahara, K., Lannuzel, D., Massom, R. A., Meiners, K. M., Swadling, K. M., Atwater, D. P., Brett, G. M., Corkill, M., Dalman, L. A., Fiddes, S., Granata, A., Guglielmo, L., Heil, P., Leonard, G. H., Mahoney, A. R., ... Wienecke, B. (2023). Antarctic Landfast Sea Ice: A Review of Its Physics, Biogeochemistry and Ecology. *Reviews of Geophysics*, 61(2), e2022RG000770. <https://doi.org/10.1029/2022RG000770>
- Golledge, N. R., Keller, E. D., Gomez, N., Naughten, K. A., Bernales, J., Trusel, L. D., & Edwards, T. L. (2019). Global environmental consequences of twenty-first-century ice-sheet melt. *Nature*, 566(7742), Article 7742. <https://doi.org/10.1038/s41586-019-0889-9>
- Haumann, F. A., Gruber, N., Münnich, M., Frenger, I., & Kern, S. (2016). Sea-ice transport driving Southern Ocean salinity and its recent trends. *Nature*, 537(7618), 89–92. <https://doi.org/10.1038/nature19101>
- Hobbs, W., Massom, R., Stammerjohn, S., Reid, P., Williams, G., & Meier, W. (2016). A review of recent changes in Southern Ocean sea ice, their drivers and forcings. *Global and Planetary Change*, 143. <https://doi.org/10.1016/j.gloplacha.2016.06.008>
- Holland, M. M., Bitz, C. M., Hunke, E. C., Lipscomb, W. H., & Schramm, J. L. (2006). Influence of the Sea Ice Thickness Distribution on Polar Climate in CCSM3. *Journal of Climate*, 19(11), 2398–2414. <https://doi.org/10.1175/JCLI3751.1>

- Holland, P. R. (2014). The seasonality of Antarctic sea ice trends. *Geophysical Research Letters*, 41(12), 4230–4237. <https://doi.org/10.1002/2014GL060172>
- Holland, P. R., & Kwok, R. (2012). Wind-driven trends in Antarctic sea-ice drift. *Nature Geoscience*, 5(12), 872–875. <https://doi.org/10.1038/ngeo1627>
- Holmes, C. R., Bracegirdle, T. J., & Holland, P. R. (2022). Antarctic Sea Ice Projections Constrained by Historical Ice Cover and Future Global Temperature Change. *Geophysical Research Letters*, 49(10), e2021GL097413. <https://doi.org/10.1029/2021GL097413>
- Holmes, C. R., Holland, P. R., & Bracegirdle, T. J. (2019). Compensating Biases and a Noteworthy Success in the CMIP5 Representation of Antarctic Sea Ice Processes. *Geophysical Research Letters*, 46(8), 4299–4307. <https://doi.org/10.1029/2018GL081796>
- Jeffery, N., Maltrud, M. E., Hunke, E. C., Wang, S., Wolfe, J., Turner, A. K., Burrows, S. M., Shi, X., Lipscomb, W. H., Maslowski, W., & Calvin, K. V. (2020). Investigating controls on sea ice algal production using E3SMv1.1-BGC. *Annals of Glaciology*, 61(82), 51–72. <https://doi.org/10.1017/aog.2020.7>
- Kay, J. E., Wall, C., Yettella, V., Medeiros, B., Hannay, C., Caldwell, P., & Bitz, C. (2016). Global Climate Impacts of Fixing the Southern Ocean Shortwave Radiation Bias in the Community Earth System Model (CESM). *Journal of Climate*, 29(12), 4617–4636. <https://doi.org/10.1175/JCLI-D-15-0358.1>
- Köhl, A. (2020). Evaluating the GECCO3 1948–2018 ocean synthesis – a configuration for initializing the MPI-ESM climate model. *Quarterly Journal of the Royal Meteorological Society*, 146(730), 2250–2273. <https://doi.org/10.1002/qj.3790>
- Kurtz, N. T., & Markus, T. (2012). Satellite observations of Antarctic sea ice thickness and volume. *Journal of Geophysical Research: Oceans*, 117(C8). <https://doi.org/10.1029/2012JC008141>
- Kusahara, K., Hasumi, H., Fraser, A. D., Aoki, S., Shimada, K., Williams, G. D., Massom, R., & Tamura, T. (2017). Modeling Ocean–Cryosphere Interactions off Adélie and George V Land, East Antarctica. *Journal of Climate*, 30(1), 163–188. <https://doi.org/10.1175/JCLI-D-15-0808.1>
- Langhorne, P. J., Squire, V. A., Fox, C., & Haskell, T. G. (1998). Break-up of sea ice by ocean waves. *Annals of Glaciology*, 27, 438–442. <https://doi.org/10.3189/S0260305500017869>
- Li, S., Zhang, Y., Chen, C., Zhang, Y., Xu, D., & Hu, S. (2023). Assessment of Antarctic Sea Ice Cover in CMIP6 Prediction with Comparison to AMSR2 during 2015–2021. *Remote Sensing*, 15(8), 2048. <https://doi.org/10.3390/rs15082048>
- Liao, S., Luo, H., Wang, J., Shi, Q., Zhang, J., & Yang, Q. (2022). An evaluation of Antarctic sea-ice thickness from the Global Ice-Ocean Modeling and Assimilation System based on in situ and satellite observations. *The Cryosphere*, 16(5), 1807–1819. <https://doi.org/10.5194/tc-16-1807-2022>
- Lindsay, R. W., & Zhang, J. (2006). Assimilation of Ice Concentration in an Ice–Ocean Model. *Journal of Atmospheric and Oceanic Technology*, 23(5), 742–749. <https://doi.org/10.1175/JTECH1871.1>
- Maksym, T., & Markus, T. (2008). Antarctic sea ice thickness and snow-to-ice conversion from atmospheric reanalysis and passive microwave snow depth. *Journal of Geophysical Research*, 113(C2), C02S12. <https://doi.org/10.1029/2006JC004085>
- Maksym, T., Stammerjohn, S., Ackley, S., & Massom, R. (2012). Antarctic Sea Ice—A Polar Opposite? *Oceanography*, 25(3), 140–151. <https://doi.org/10.5670/oceanog.2012.88>

- Massom, R. A., & Stammerjohn, S. E. (2010). Antarctic sea ice change and variability – Physical and ecological implications. *Polar Science*, 4(2), 149–186.
<https://doi.org/10.1016/j.polar.2010.05.001>
- Massonnet, F., Mathiot, P., Fichefet, T., Goosse, H., König Beatty, C., Vancoppenolle, M., & Lavergne, T. (2013). A model reconstruction of the Antarctic sea ice thickness and volume changes over 1980–2008 using data assimilation. *Ocean Modelling*, 64, 67–75.
<https://doi.org/10.1016/j.ocemod.2013.01.003>
- Notz, D., & Community, S. (2020). Arctic Sea Ice in CMIP6. *Geophysical Research Letters*, 47(10), e2019GL086749. <https://doi.org/10.1029/2019GL086749>
- Parkinson, C. L., & Cavalieri, D. J. (2012). Antarctic sea ice variability and trends, 1979–2010. *The Cryosphere*, 6(4), 871–880. <https://doi.org/10.5194/tc-6-871-2012>
- Paul, S., Hendricks, S., Ricker, R., Kern, S., & Rinne, E. (2018). Empirical parametrization of Envisat freeboard retrieval of Arctic and Antarctic sea ice based on CryoSat-2: Progress in the ESA Climate Change Initiative. *The Cryosphere*, 12. <https://doi.org/10.5194/tc-12-2437-2018>
- Pelichero, V., Sallée, J.-B., Chapman, C. C., & Downes, S. M. (2018). The southern ocean meridional overturning in the sea-ice sector is driven by freshwater fluxes. *Nature Communications*, 9(1), 1789. <https://doi.org/10.1038/s41467-018-04101-2>
- Poulsen, M. B., Jochum, M., & Nuterman, R. (2018). Parameterized and resolved Southern Ocean eddy compensation. *Ocean Modelling*, 124, 1–15.
<https://doi.org/10.1016/j.ocemod.2018.01.008>
- Purich, A., & England, M. H. (2023). Projected Impacts of Antarctic Meltwater Anomalies over the Twenty-First Century. *Journal of Climate*, 36(8), 2703–2719.
<https://doi.org/10.1175/JCLI-D-22-0457.1>
- Rackow, T., Sein, D. V., Semmler, T., Danilov, S., Koldunov, N. V., Sidorenko, D., Wang, Q., & Jung, T. (2019). Sensitivity of deep ocean biases to horizontal resolution in prototype CMIP6 simulations with AWI-CM1.0. *Geoscientific Model Development*, 12(7), 2635–2656. <https://doi.org/10.5194/gmd-12-2635-2019>
- Roach, L. A., Dörr, J., Holmes, C. R., Massonnet, F., Blockley, E. W., Notz, D., Rackow, T., Raphael, M. N., O'Farrell, S. P., Bailey, D. A., & Bitz, C. M. (2020). Antarctic Sea Ice Area in CMIP6. *Geophysical Research Letters*, 47(9), e2019GL086729.
<https://doi.org/10.1029/2019GL086729>
- Sallée, J. B., Abrahamsen, E. P., Allaire, C., Auger, M., Ayres, H., Badhe, R., Boutin, J., Brearley, J. A., de Lavergne, C., ten Doeschate, A. M. M., Droste, E. S., du Plessis, M. D., Ferreira, D., Giddy, I. S., Gülk, B., Gruber, N., Hague, M., Hoppema, M., Josey, S. A., ... Zhou, S. (n.d.). Southern ocean carbon and heat impact on climate. *Philosophical Transactions. Series A, Mathematical, Physical, and Engineering Sciences*, 381(2249), 20220056. <https://doi.org/10.1098/rsta.2022.0056>
- Schultz, C. (2013). Antarctic sea ice thickness affects algae populations. *Eos, Transactions American Geophysical Union*, 94. <https://doi.org/10.1002/2013EO030032>
- Schwegmann, S., Rinne, E., Ricker, R., Hendricks, S., & Helm, V. (2016). About the consistency between Envisat and CryoSat-2 radar freeboard retrieval over Antarctic sea ice. *The Cryosphere*, 10(4), 1415–1425. <https://doi.org/10.5194/tc-10-1415-2016>
- Shi, Q., Yang, Q., Mu, L., Wang, J., Massonnet, F., & Mazloff, M. R. (2021). Evaluation of sea-ice thickness from four reanalyses in the Antarctic Weddell Sea. *The Cryosphere*, 15(1), 31–47. <https://doi.org/10.5194/tc-15-31-2021>

- Shu, Q., Song, Z., & Qiao, F. (2015). Assessment of sea ice simulations in the CMIP5 models. *The Cryosphere*, 9(1), 399–409. <https://doi.org/10.5194/tc-9-399-2015>
- Shu, Q., Wang, Q., Song, Z., Qiao, F., Zhao, J., Chu, M., & Li, X. (2020). Assessment of Sea Ice Extent in CMIP6 With Comparison to Observations and CMIP5. *Geophysical Research Letters*, 47(9), e2020GL087965. <https://doi.org/10.1029/2020GL087965>
- Singh, H. K. A., Landrum, L., Holland, M. M., Bailey, D. A., & DuVivier, A. K. (2021). An Overview of Antarctic Sea Ice in the Community Earth System Model Version 2, Part I: Analysis of the Seasonal Cycle in the Context of Sea Ice Thermodynamics and Coupled Atmosphere-Ocean-Ice Processes. *Journal of Advances in Modeling Earth Systems*, 13(3), e2020MS002143. <https://doi.org/10.1029/2020MS002143>
- Stammerjohn, S., Martinson, D., Smith, R., Yuan, X., & Rind, D. (2008). Trends in Antarctic annual sea ice retreat and advance and their relation to El Niño-Southern Oscillation and Southern Annular Mode variability. *Journal of Geophysical Research: Oceans*, 113.
- St-Laurent, P., Yager, P. L., Sherrell, R. M., Stammerjohn, S. E., & Dinniman, M. S. (2017). Pathways and supply of dissolved iron in the Amundsen Sea (Antarctica). *Journal of Geophysical Research: Oceans*, 122(9), 7135–7162. <https://doi.org/10.1002/2017JC013162>
- Stroeve, J., Barrett, A., Serreze, M., & Schweiger, A. (2014). Using records from submarine, aircraft and satellites to evaluate climate model simulations of Arctic sea ice thickness. *The Cryosphere*, 8(5), 1839–1854. <https://doi.org/10.5194/tc-8-1839-2014>
- Tilling, R., Ridout, A., & Shepherd, A. (2019). Assessing the Impact of Lead and Floe Sampling on Arctic Sea Ice Thickness Estimates from Envisat and CryoSat-2. *Journal of Geophysical Research: Oceans*, 124(11), Article 11.
- Turner, J., Bracegirdle, T. J., Phillips, T., Marshall, G. J., & Hosking, J. S. (2013). An Initial Assessment of Antarctic Sea Ice Extent in the CMIP5 Models. *Journal of Climate*, 26(5), 1473–1484. <https://doi.org/10.1175/JCLI-D-12-00068.1>
- Turner, J., Hosking, J. S., Bracegirdle, T. J., Marshall, G. J., & Phillips, T. (2015). Recent changes in Antarctic Sea Ice. *Philosophical Transactions of the Royal Society A: Mathematical, Physical and Engineering Sciences*, 373(2045), 20140163. <https://doi.org/10.1098/rsta.2014.0163>
- Uotila, P., Holland, P. R., Vihma, T., Marsland, S. J., & Kimura, N. (2014). Is realistic Antarctic sea-ice extent in climate models the result of excessive ice drift? *Ocean Modelling*, 79, 33–42. <https://doi.org/10.1016/j.ocemod.2014.04.004>
- Van Achter, G., Fichefet, T., Goosse, H., Pelletier, C., Sterlin, J., Huot, P.-V., Lemieux, J.-F., Fraser, A. D., Haubner, K., & Porter-Smith, R. (2022). Modelling landfast sea ice and its influence on ocean–ice interactions in the area of the Totten Glacier, East Antarctica. *Ocean Modelling*, 169, 101920. <https://doi.org/10.1016/j.ocemod.2021.101920>
- Vernet, M., Geibert, W., Hoppema, M., Brown, P. J., Haas, C., Hellmer, H. H., Jokat, W., Jullion, L., Mazloff, M., Bakker, D. C. E., Brearley, J. A., Croot, P., Hattermann, T., Hauck, J., Hillenbrand, C.-D., Hoppe, C. J. M., Huhn, O., Koch, B. P., Lechtenfeld, O. J., ... Verdy, A. (2019). The Weddell Gyre, Southern Ocean: Present Knowledge and Future Challenges. *Reviews of Geophysics*, 57(3), 623–708. <https://doi.org/10.1029/2018RG000604>
- Wang, J., Min, C., Ricker, R., Shi, Q., Han, B., Hendricks, S., Wu, R., & Yang, Q. (2022). A comparison between Envisat and ICESat sea ice thickness in the Southern Ocean. *The Cryosphere*, 16(10), 4473–4490. <https://doi.org/10.5194/tc-16-4473-2022>

- Willatt, R. C., Giles, K. A., Laxon, S. W., Stone-Drake, L., & Worby, A. P. (2010). Field Investigations of Ku-Band Radar Penetration Into Snow Cover on Antarctic Sea Ice. *IEEE Transactions on Geoscience and Remote Sensing*, 48(1), 365–372. <https://doi.org/10.1109/TGRS.2009.2028237>
- Worby, A. P., Geiger, C. A., Paget, M. J., Woert, M. L. V., Ackley, S. F., & DeLiberty, T. L. (2008). Thickness distribution of Antarctic sea ice. *Journal of Geophysical Research: Oceans*, 113(C5). <https://doi.org/10.1029/2007JC004254>
- Xu, Y., Li, H., Liu, B., Xie, H., & Ozsoy-Cicek, B. (2021). Deriving Antarctic Sea-Ice Thickness From Satellite Altimetry and Estimating Consistency for NASA's ICESat/ICESat-2 Missions. *Geophysical Research Letters*, 48(20), e2021GL093425. <https://doi.org/10.1029/2021GL093425>
- Zelinka, M. D., Myers, T. A., McCoy, D. T., Po-Chedley, S., Caldwell, P. M., Ceppi, P., Klein, S. A., & Taylor, K. E. (2020). Causes of Higher Climate Sensitivity in CMIP6 Models. *Geophysical Research Letters*, 47(1), e2019GL085782. <https://doi.org/10.1029/2019GL085782>
- Zhang, J. (2014). Modeling the Impact of Wind Intensification on Antarctic Sea Ice Volume. *Journal of Climate*, 27(1), 202–214. <https://doi.org/10.1175/JCLI-D-12-00139.1>
- Zhang, J., & Rothrock, D. A. (2003). Modeling Global Sea Ice with a Thickness and Enthalpy Distribution Model in Generalized Curvilinear Coordinates. *Monthly Weather Review*, 131(5), 845–861. [https://doi.org/10.1175/1520-0493\(2003\)131<0845:MGSIWA>2.0.CO;2](https://doi.org/10.1175/1520-0493(2003)131<0845:MGSIWA>2.0.CO;2)
- Zwally, H. J., Comiso, J. C., Parkinson, C. L., Cavalieri, D. J., & Gloersen, P. (2002). Variability of Antarctic sea ice 1979–1998. *Journal of Geophysical Research: Oceans*, 107(C5), 9-1–9–19. <https://doi.org/10.1029/2000JC000733>

References for Supporting Material:

- Cherchi, A., Fogli, P. G., Lovato, T., Peano, D., Iovino, D., Gualdi, S., Masina, S., Scoccimarro, E., Materia, S., Bellucci, A., & Navarra, A. (2019). Global Mean Climate and Main Patterns of Variability in the CMCC-CM2 Coupled Model. *Journal of Advances in Modeling Earth Systems*, 11(1), 185–209. <https://doi.org/10.1029/2018MS001369>
- Counillon, F., Keenlyside, N., Bethke, I., Wang, Y., Billeau, S., Shen, M.-L., & Bentsen, M. (2016). Flow-dependent assimilation of sea surface temperature in isopycnal coordinates with the Norwegian Climate Prediction Model. *Tellus A*, 68. <https://doi.org/10.3402/tellusa.v68.32437>
- Danabasoglu, G., Lamarque, J.-F., Bacmeister, J., Bailey, D. A., DuVivier, A. K., Edwards, J., Emmons, L. K., Fasullo, J., Garcia, R., Gettelman, A., Hannay, C., Holland, M. M., Large, W. G., Lauritzen, P. H., Lawrence, D. M., Lenaerts, J. T. M., Lindsay, K., Lipscomb, W. H., Mills, M. J., ... Strand, W. G. (2020). The Community Earth System Model Version 2 (CESM2). *Journal of Advances in Modeling Earth Systems*, 12(2), e2019MS001916. <https://doi.org/10.1029/2019MS001916>
- Döscher, R., Acosta, M., Alessandri, A., Anthoni, P., Arsouze, T., Bergman, T., Bernardello, R., Boussetta, S., Caron, L.-P., Carver, G., Castrillo, M., Catalano, F., Cvijanovic, I., Davini, P., Dekker, E., Doblas-Reyes, F. J., Docquier, D., Echevarria, P., Fladrich, U., ... Zhang, Q. (2022). The EC-Earth3 Earth system model for the Coupled Model Intercomparison

- Project 6. Geoscientific Model Development, 15(7), 2973–3020.
<https://doi.org/10.5194/gmd-15-2973-2022>
- Gettelman, A., Mills, M. J., Kinnison, D. E., Garcia, R. R., Smith, A. K., Marsh, D. R., Tilmes, S., Vitt, F., Bardeen, C. G., McInerney, J., Liu, H., Solomon, S. C., Polvani, L. M., Emmons, L. K., Lamarque, J., Richter, J. H., Glanville, A. S., Bacmeister, J. T., Phillips, A. S., ... Randel, W. J. (2019). The Whole Atmosphere Community Climate Model Version 6 (WACCM6). *Journal of Geophysical Research: Atmospheres*, 124(23), Article 23.
- Gutjahr, O., Putrasahan, D., Lohmann, K., Jungclaus, J. H., von Storch, J.-S., Brüggemann, N., Haak, H., & Stössel, A. (2019). Max Planck Institute Earth System Model (MPI-ESM1.2) for the High-Resolution Model Intercomparison Project (HighResMIP). *Geoscientific Model Development*, 12(7), 3241–3281. <https://doi.org/10.5194/gmd-12-3241-2019>
- Held, I. M., Guo, H., Adcroft, A., Dunne, J. P., Horowitz, L. W., Krasting, J., Shevliakova, E., Winton, M., Zhao, M., Bushuk, M., Wittenberg, A. T., Wyman, B., Xiang, B., Zhang, R., Anderson, W., Balaji, V., Donner, L., Dunne, K., Durachta, J., ... Zadeh, N. (2019). Structure and Performance of GFDL's CM4.0 Climate Model. *Journal of Advances in Modeling Earth Systems*, 11(11), 3691–3727. <https://doi.org/10.1029/2019MS001829>
- Lin, Y., Huang, X., Liang, Y., Qin, Y., Xu, S., Huang, W., Xu, F., Liu, L., Wang, Y., Peng, Y., Wang, L., Xue, W., Fu, H., Zhang, G. J., Wang, B., Li, R., Zhang, C., Lu, H., Yang, K., ... Gong, P. (2020). Community Integrated Earth System Model (CIESM): Description and Evaluation. *Journal of Advances in Modeling Earth Systems*, 12(8), e2019MS002036. <https://doi.org/10.1029/2019MS002036>
- Lurton, T., Balkanski, Y., Bastrikov, V., Bekki, S., Bopp, L., Braconnot, P., Brockmann, P., Cadule, P., Contoux, C., Cozic, A., Cugnet, D., Dufresne, J.-L., Éthé, C., Foujols, M.-A., Ghattas, J., Hauglustaine, D., Hu, R.-M., Kageyama, M., Khodri, M., ... Boucher, O. (2020). Implementation of the CMIP6 Forcing Data in the IPSL-CM6A-LR Model. *Journal of Advances in Modeling Earth Systems*, 12(4), e2019MS001940. <https://doi.org/10.1029/2019MS001940>
- Massonnet, F., Ménégoz, M., Acosta, M., Yépez-Arbós, X., Exarchou, E., & Doblas-Reyes, F. J. (2020). Replicability of the EC-Earth3 Earth system model under a change in computing environment. *Geoscientific Model Development*, 13(3), 1165–1178. <https://doi.org/10.5194/gmd-13-1165-2020>
- Mauritsen, T., Bader, J., Becker, T., Behrens, J., Bittner, M., Brokopf, R., Brovkin, V., Claussen, M., Crueger, T., Esch, M., Fast, I., Fiedler, S., Fläschner, D., Gayler, V., Giorgi, M., Goll, D. S., Haak, H., Hagemann, S., Hedemann, C., ... Roeckner, E. (2019). Developments in the MPI-M Earth System Model version 1.2 (MPI-ESM1.2) and Its Response to Increasing CO₂. *Journal of Advances in Modeling Earth Systems*, 11(4), 998–1038. <https://doi.org/10.1029/2018MS001400>
- Park, S., Shin, J., Kim, S., Oh, E., & Kim, Y. (2019). Global Climate Simulated by the Seoul National University Atmosphere Model Version 0 with a Unified Convection Scheme (SAM0-UNICON). *Journal of Climate*, 32. <https://doi.org/10.1175/JCLI-D-18-0796.1>
- Seland, Ø., Bentsen, M., Olivié, D., Toniazzo, T., Gjermundsen, A., Graff, L. S., Debernard, J. B., Gupta, A. K., He, Y.-C., Kirkevåg, A., Schwinger, J., Tjiputra, J., Aas, K. S., Bethke, I., Fan, Y., Griesfeller, J., Grini, A., Guo, C., Ilicak, M., ... Schulz, M. (2020). Overview of the Norwegian Earth System Model (NorESM2) and key climate response of CMIP6

- DECK, historical, and scenario simulations. *Geoscientific Model Development*, 13(12), 6165–6200. <https://doi.org/10.5194/gmd-13-6165-2020>
- Tatebe, H., Ogura, T., Nitta, T., Komuro, Y., Ogochi, K., Takemura, T., Sudo, K., Sekiguchi, M., Abe, M., Saito, F., Chikira, M., Watanabe, S., Mori, M., Hirota, N., Kawatani, Y., Mochizuki, T., Yoshimura, K., Takata, K., O’ishi, R., ... Kimoto, M. (2019). Description and basic evaluation of simulated mean state, internal variability, and climate sensitivity in MIROC6. *Geoscientific Model Development*, 12(7), 2727–2765. <https://doi.org/10.5194/gmd-12-2727-2019>
- van Noije, T., Bergman, T., Le Sager, P., O’Donnell, D., Makkonen, R., Gonçalves-Ageitos, M., Döscher, R., Fladrich, U., von Hardenberg, J., Keskinen, J.-P., Korhonen, H., Laakso, A., Myriokefalitakis, S., Ollinaho, P., Pérez García-Pando, C., Reerink, T., Schrödner, R., Wyser, K., & Yang, S. (2021). EC-Earth3-AerChem: A global climate model with interactive aerosols and atmospheric chemistry participating in CMIP6. *Geoscientific Model Development*, 14(9), 5637–5668. <https://doi.org/10.5194/gmd-14-5637-2021>
- Wyser, K., van Noije, T., Yang, S., von Hardenberg, J., O’Donnell, D., & Döscher, R. (2020). On the increased climate sensitivity in the EC-Earth model from CMIP5 to CMIP6. *Geoscientific Model Development*, 13(8), 3465–3474. <https://doi.org/10.5194/gmd-13-3465-2020>
- Yukimoto, S., Kawai, H., Koshiro, T., Oshima, N., Yoshida, K., Urakawa, S., Tsujino, H., Deushi, M., Tanaka, T., Hosaka, M., Yabu, S., Yoshimura, H., Shindo, E., Mizuta, R., Obata, A., Adachi, Y., & Ishii, M. (2019). The Meteorological Research Institute Earth System Model Version 2.0, MRI-ESM2.0: Description and Basic Evaluation of the Physical Component. *Journal of the Meteorological Society of Japan. Ser. II*, 97(5), 931–965. <https://doi.org/10.2151/jmsj.2019-051>
- Ziehn, T., Chamberlain, M. A., Law, R. M., Lenton, A., Bodman, R. W., Dix, M., Stevens, L., Wang, Y.-P., Srbinovsky, J., Ziehn, T., Chamberlain, M. A., Law, R. M., Lenton, A., Bodman, R. W., Dix, M., Stevens, L., Wang, Y.-P., & Srbinovsky, J. (2020). The Australian Earth System Model: ACCESS-ESM1.5. *Journal of Southern Hemisphere Earth Systems Science*, 70(1), 193–214. <https://doi.org/10.1071/ES19035>